RANDOM SUBSPACE METHOD FOR SOURCE CAMERA IDENTIFICATION

Ruizhe Li[1], *Constantine Kotropoulos*[2], *Chang-Tsun Li*[1], *and Yu Guan*[1]

[1]Department of Computer Science, University of Warwick, Coventry, CV4 7AL, UK
[2]Department of Informatics, Aristotle University of Thessaloniki, Thessaloniki, 54124, Greece

ABSTRACT

Sensor Pattern Noise is an inherent fingerprint of imaging devices, which has been widely used for source camera identification, image classification, and forgery detection. In a previous work, we proposed a feature extraction method based on the principal component analysis denoising concept, which can enhance the performance of conventional SPN extraction methods. However, this method is vulnerable, because the training samples are seriously affected by the image content. Accordingly, it is difficult to train a reliable feature extractor by using such a training set. To address this problem, a camera identification framework based on the random subspace method and majority voting is proposed in this work. The experimental results show that the proposed solution can suppress the interference from scene details and enhance the performance in terms of the receiver operating characteristic curve.

Index Terms**—** Digital forensics, Sensor pattern noise, PCA denoising, Random subspace method

1. INTRODUCTION

Digital images are more and more frequently used as evidences in court to support judgements. For example, forensic investigators need to identify the origin of the digital images in order to link the images to the cameras that acquired them, such as child pornography and movie piracy. Therefore, effective techniques for identifying the origin of digital images are urgently needed.

Sensor pattern noise (SPN) has been proved as a reliable *fingerprint* of imaging device to solve the camera identification problem. There have been several works made in the SPN-based camera identification field. The tasks for camera identification can be broadly split into three steps: 1) The first step is the SPN extraction from the query image. Lukas *et al.* [1] first proposed using SPN extracted from digital image to trace back the imaging device. They adopted a wavelet-based Wiener filter to extract the SPN from wavelet high frequency coefficients. After that, Dabov *et al.* [2] proposed a sparse 3D transform-domain collaborative filtering to extract SPN. In [3], Chen *et al.* proposed a maximum likelihood estimation method to estimate the corresponding multiplicative factor from the reference images. In [4], Li introduced a SPN enhancer to suppress the contamination caused by image content. A further investigation into SPN's location-dependent quality is reported by Li and Satta in [5]. In [6], Li *et al.* proposed a colour-decoupled SPN extraction method to prevent the color filter array interpolation noise from propagating into the physical components. In [7], Kang *et al.* introduced a context adaptive SPN predictor to suppress the impact of image content. 2) The second step is to estimate the reference SPN from the suspect camera. A camera reference SPN is usually built by averaging SPNs extracted from multiple low-variation images taken by the same camera. In [8], Li *et al.* proposed a reference SPN estimator which is able to estimate a reliable reference from natural images with varying scene details. 3) The final step is to detect whether the query SPN correlates to the reference camera SPN. Normalized cross-correlation is usually adopted as the detector [1]. Later, Goljan *et al.* [9] introduced the peak to correlation energy ratio as a replacement for the normalized correlation. Another detection statistic correlation over circular correlation norm is proposed by Kang *et al.* [10].

Some consideration has been given to source camera identification against the large database, where the goal is to match a sensor fingerprint to a large number of fingerprints in a database. This capability is needed when one needs to attribute one or more images from an unknown camera to a large number of images in a large image repository to find other images that may have been taken from the same camera. In this case, the high dimensionality of SPN fingerprint will incur an expensive computational cost in the matching phase and exorbitant storage requirements. To solve this problem, Goljan *et al.* [11] proposed a fingerprint digest, which is formed by keeping only a small number of the largest fingerprint values and their positions. Later, Hu *et al.* [12] proposed a fast fingerprint digest search algorithm to further improve the identification efficiency. In [13], Bayram *et al.* proposed to represent a sensor fingerprint in binary-quantized form, which speeds-up the correlation detection and also greatly reduces the size of fingerprint.

Recently, Li *et al.* [14] proposed a feature extractor based on the Principal Component Analysis (PCA) denoising [15] to extract a small feature set, which contains most of the discriminative information of the SPN fingerprint.

This method can significantly improve several existing SPN extraction methods in the literature and achieve the state-of-the-art Receiver Operating Characteristic (ROC) curve performance. However, this improvement will degrade because the training samples are seriously affected by the scene details. To solve this problem in this paper, a solution based on the Random Subspace Method (RSM) and Majority Voting (MV) is proposed. The rest of this paper is organized as follows. In Section 2, we introduce the way to construct the entire feature space and describe how to conduct an ensemble method based on the RSM and MV in the context of source camera identification. Experimental results are reported in Section 3. Finally, conclusion is drawn in Section 4.

2. PROPOSED METHOD

In [15] PCA denoising was introduced to the SPN-based source camera identification. Based on this concept, a feature extractor was proposed to extract SPN components from the original noise residual. By using noise residuals extracted only from low-variation reference images (*i.e.,* blue sky images) as training samples, such a feature extractor can be learned and optimized for SPN extraction. This optimized feature extractor is able to suppress the redundancy and interfering components (*e.g.,* color interpolation, JPEG compression, distortion introduced by denoising filter) in the real SPN signal.

However, an effective feature extractor can only be learned based on a representative training set, while this assumption may not hold in real-world scenarios. For example, an investigator may just have reference images of a camera from Facebook or Flickr for training, which are more likely natural images with varying scene details rather than blue sky images. However, the SPN is a subtle signal, which can be severely contaminated by scene details. The magnitude of scene details tends to be far greater than that of the real SPN, as demonstrated in Fig. 1(b). In this case, the leading eigenvectors of the learned feature extractor is more likely to represent the scene details rather than the real SPN. Here, to build a model that generalizes to training samples with varying scene details, we propose a solution based on the random subspace method.

2.1. Feature space construction

Assume there are n images $\{I_i\}_{i=1}^n$ taken by c cameras $\{C_j\}_{j=1}^c$ in the database and each camera has taken E_j images. We first extract noise residuals from $N \times N$-pixels blocks cropped from the centre of these full-sized images denoted as $\{\boldsymbol{x}_i \in \mathbb{R}^{N \times N}\}_{i=1}^n$. These n SPN templates form the training set. PCA is performed to seek a set of orthonormal vectors $\boldsymbol{v}_k$ and their associated eigenvalues λ_k of the covariance matrix S

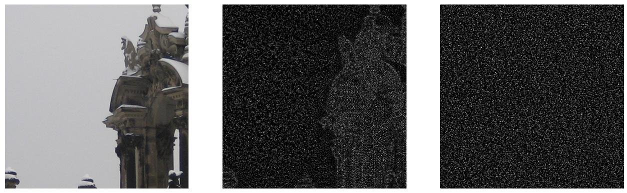

(a) (b) (c)

Fig. 1: (a) An image taken by Canon Ixus70. (b) he noise residual extracted from (a) which is contaminated by scene details. (c) Clean reference SPN of Canon Ixus70. (Note the intensity of these image has been scaled to the interval [0,255] for visualization purpose.)

$$S = \frac{1}{n}\sum_{i=1}^{n} \boldsymbol{x}_i \boldsymbol{x}_i^T = AA^T \tag{1}$$

where $A = \frac{1}{\sqrt{n}}[\boldsymbol{x}_1, \ldots, \boldsymbol{x}_n] \in \mathbb{R}^{N^2 \times n}$. Notice that the dimensionality of SPN could be extremely high (*e.g.,* N^2=1024^2). Therefore, directly solving the eigenvalue decomposition problem of $S \in \mathbb{R}^{N^2 \times N^2}$ incurs a prohibitive computational cost (with a complexity $O(N^6)$). To make PCA feasible for the high-dimensional SPN, we apply instead a fast method of computing these eigenvectors (when $n \ll N^2$). Assume $\boldsymbol{v}_k{}'$ is the unit eigenvector of $A^T A \in \mathbb{R}^{n \times n}$ with eigenvalue λ_k'. We could obtain $A^T A \boldsymbol{v}_k{}' = \lambda_k{}' \boldsymbol{v}_k{}'$. Multiplying both sides by A, we have $AA^T(A\boldsymbol{v}_k{}') = \lambda_k{}'(A\boldsymbol{v}_k{}')$, where $A\boldsymbol{v}_k{}'$ are the eigenvectors of $AA^T = S$ with eigenvalues $\lambda_k{}'$. Thus, instead of solving the eigenvalue decomposition of matrix S directly, we can calculate the eigenvectors $\boldsymbol{v}_k{}'$ via the smaller matrix $A^T A \in \mathbb{R}^{n \times n}$ and obtain the objective $\boldsymbol{v}_k$ by $\boldsymbol{v}_k = A\boldsymbol{v}_k{}'$. The obtained $\{\boldsymbol{v}_k\}_{k=1}^n$ are then normalized and sorted in the descending order according to their associated eigenvalues $\lambda_1 \geq \lambda_2 \geq ...\lambda_n$. Note that only when $n \ll N^2$, computing eigenvectors via this method (with a complexity $O(n^3)$) would be more effective than the traditional way. The top d=$\min\{d' | \sum_{i=1}^{d'} \lambda_i / \sum_{i=1}^{n} \lambda_i > 99\%\}$ eigenvectors with non-zero eigenvalues are then retained as the feature space $T = [\boldsymbol{u}_1, ..., \boldsymbol{u}_d] \in \mathbb{R}^{N^2 \times d}$.

If the training samples contain scene details, there will be some leading eigenvectors in the feature space T that represent the scene details rather than the real SPN signal. Therefore, it is hard for the previous PCA-based feature extractor [14] to preserve the SPN identification accuracy when scene details are involved in the training set. Moreover, in real applications, the training samples tend to depict a wide variety of natural scenes. As a result, the corrupted eigenvectors caused by these scene details are hard to be located in the feature space T, since the scene details may differ across different training samples and will not have a fixed structure. Accordingly, this problem can not be simply solved by removing some special eigenvectors from the feature space. To address this problem, we propose to randomly select subsets from the feature space T to suppress the effect of scene details.

2.2. Random subspace construction

The random subspace method has been successfully applied in face recognition [6] and gait recognition [16]. Motivated by [6, 16], in this work we explore such technique in the context of source camera identification.

Each eigenvector in feature subspace T is a candidate to build the random subspaces. A random subspace R can be constructed by randomly selecting several eigenvectors from these candidates. By repeating L times the process of randomly selecting subsets of T (with size $M < d$), the random subspaces $\{R^l \in \mathbb{R}^{N\times M}\}_{l=1}^{L}$ are generated and can be used as random feature extractors. Then, a SPN template can be represented as a set of random features, such as

$$\boldsymbol{y}^l = \boldsymbol{x}R^l, l = 1, 2, ..., L, \tag{2}$$

where $\boldsymbol{y}^l$ is a new representation for the SPN $\boldsymbol{x}$ in the subspace R^l. After the just described approach, each SPN $\boldsymbol{x}$ can be represented as a set of projected vectors $\{\boldsymbol{y}^l\}_{l=1}^{L}$ corresponding to L d-dimensional random subspaces, which can be used as features for further processing.

2.3. Camera identification via majority voting

For a query SPN sample, after extracting its features from the aforementioned subspaces, the following steps can be adopted to detect whether this query sample is taken by a specific camera in the database.

1) Reference estimation. By performing the random subspace feature extraction on the training samples $\{\boldsymbol{x}_i\}_{i=1}^{n}$, we can generate a set of features $\{y_i^l\}_{i=1}^{n}$ in each random subspace R^l. The reference $\boldsymbol{y'}_j^l$ of the camera C_j in the subspace R^l then can be estimated by averaging all the features belong to that camera as

$$\boldsymbol{y'}_j^l = \frac{\sum_{i=1}^{E_j} \boldsymbol{y}_i^l}{E_j}, j = 1, 2, ..., c \tag{3}$$

2) Identification. Let $\boldsymbol{x}_q$ be a query SPN vector. By applying (2), a set of features $\{\boldsymbol{y}_q^l\}_{l=1}^{L}$ are obtained. Once the query feature $\boldsymbol{y}_q^l$ and the camera's reference SPN $\boldsymbol{y'}_j^l$ are generated, the camera identification problem can be modeled as a two-channel hypothesis problem

$$\begin{aligned} &H_0 : \boldsymbol{y}_q^l \neq \boldsymbol{y'}_j^l \text{(the query image is not taken by the } j\text{th camera)} \\ &H_1 : \boldsymbol{y}_q^l = \boldsymbol{y'}_j^l \text{(the query image is taken by the } j\text{th camera)} \end{aligned} \tag{4}$$

Then, a correlation-based detector will be established to make the decision between H_0 and H_1 by comparing the correlation $\rho = corr(\boldsymbol{y}_q^l, \boldsymbol{y'}_j^l)$ to a threshold t. The detector decides H_1 when $\rho \geq t$ and decides H_0 when $\rho < t$. In this paper, the Normalized Cross-Correlation (NCC) [1] is adopted as the detection statistic to measure the similarity between the query feature $\boldsymbol{y}_q^l$ and the reference feature $\boldsymbol{y'}_j^l$.

3) Majority voting. In each subspace R^l, the aforementioned identification process will be performed once. Every decision between H_0 and H_1 will be made based on the comparison between $corr(\boldsymbol{y}_q^l, \boldsymbol{y'}_j^l)$ and a fixed pre-calculated threshold t. By repeating this process in every subspace, L decisions will be obtained in total. Then, the final decision can be achieved according to the majority voting among these L decisions. For example, if more than $L/2$ decisions are voted for H_1, the final decision will assert that the query image is taken by this camera.

3. EXPERIMENTS

3.1. Experimental setup

In this work, the noise residuals extracted by the methods of Lukas [1] and Kang [7] are used as original features. In order to evaluate the feasibility of the proposed method, these original features are given as inputs to the PCA-based feature extraction method [14] and the proposed method for the performance comparison. Hereafter, Lukas/Kang+PCA and Lukas/Kang+RSM indicate that the noise residuals are firstly extracted by Lukas/Kang method and the PCA-based feature extraction or the proposed RSM is performed afterwards. Our experiments are conducted on the Dresden Image database [17]. A total of 1200 images from 10 cameras are involved in the experiment, where each responsible for 120. These 10 camera devices belong to 4 camera models, each camera model has 2∼3 different devices. The cameras are listed in Table 1. All these images are natural images containing a wide variety of natural indoor and outdoor scenes. For each camera, 20 images are used for training and the remaining 100 are used as query images for testing. Thus, there are 100×10 intraclass and 900×10 interclass correlation values in total. We extract all the noise residuals from the luminance channel, as the luminance channel contains information of all the three channels. Our experiments are performed on an image block of 256×256 pixels cropped from the centre of a full size image.

Table 1: Cameras used in the experiments

Cameras	**Alias**	**Resolution**
Canon_Ixus70_A	C11	3072×2304
Canon_Ixus70_B	C12	3072×2304
Canon_Ixus70_C	C13	3072×2304
Nikon_CoolPixS710_A	C21	4352×3264
Nikon_CoolPixS710_B	C22	4352×3264
Samsung_L74wide_A	C31	3072×2304
Samsung_L74wide_B	C32	3072×2304
Samsung_L74wide_C	C33	3072×2304
Olympus_mju_1050SW_A	C41	3648×2736
Olympus_mju_1050SW_B	C42	3648×2736

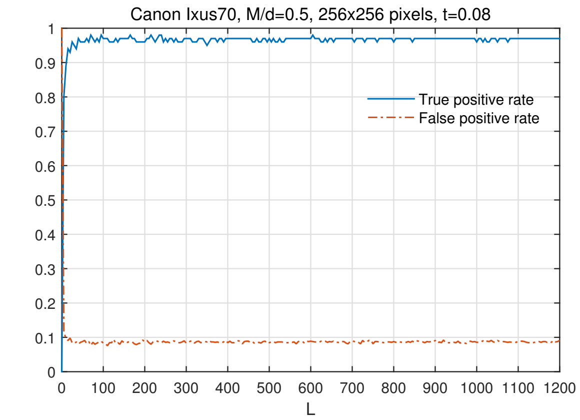

Fig. 2: Performance with respect to the number of random subspaces L.

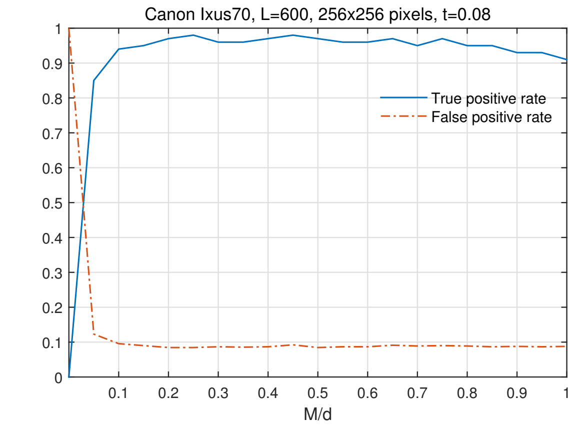

Fig. 3: Performance with respect to the dimension of the random subspace M.

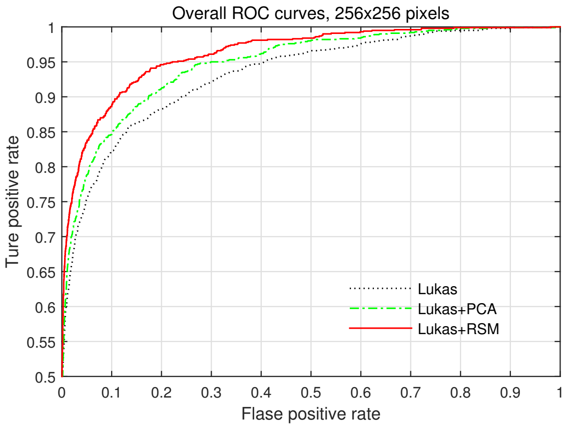

Fig. 4: ROC curves of different variants of Lukas' method [1].

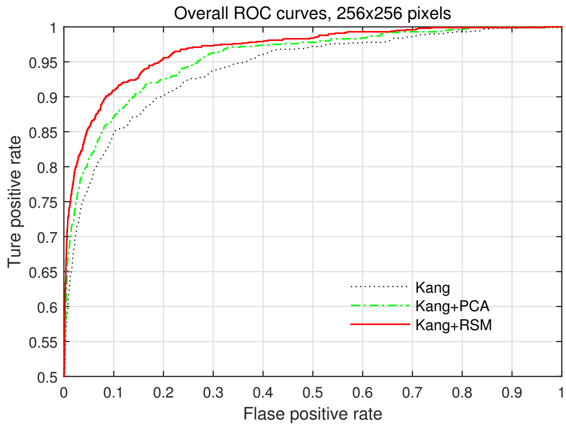

Fig. 5: ROC curves of different variants of Kang's method [7].

3.2. Performance evaluation

There are only two parameters in the proposed method, namely, the dimension of random subspace M and the number of random subspaces L. Figs. 2 and 3 show how the true positive (false positive) rate of the method Lukas+RSM vary for different values of M and L, respectively. As shown in Fig. 2, the performance of the proposed method improves by increasing number of random subspaces. Since the performance tends to be stable when $L > 600$ and there is a tradeoff between the performance and the computational cost, we set $L = 600$ in the following experiments.

Fig. 3 indicates the sensitivity of the proposed method to the parameter M. It is worth mentioning that the performance of the proposed method and the PCA-based extraction method [14] will be exactly the same, when $M/d = 1$, where d is dimension of PCA feature. Therefore, from Fig. 3 we can see that as long as $M < d$, the proposed method can achieve a higher true positive rate than the PCA-based method. In addition, from both Figs. 2 and 3 we can see that the performance of the proposed method is not sensitive to L and M. In rest of this paper, we empirically set $L = 600$ and $M/d = 0.5$, because these values yield the best result.

We use the Receiver Operating Characteristic (ROC) curve to compare the performance of different methods, as shown in Figs. 4 and 5. To get convincing results, all the 100×10 intraclass and 900×10 interclass samples from 10 cameras are used together to draw the overall ROC curve [7]. However, the overall ROC curve for the proposed method is obtained in a slightly different manner. For a given detection threshold, we count the number of true positive decisions and the number of false positive decisions for each camera in each subspace, respectively and then sum them up to obtain the total number of true positive decisions and false positive decisions. Finally, the total True Positive Rate and total False Positive Rate are calculated to draw the overall ROC curve. In Figs. 4 and 5, the black, blue, and red lines indicate the ROC curve of the Lukas/Kang, Lukas/Kang+PCA, and Lukas/Kang+RSM methods, respectively. As can be seen from Figs. 4 and 5, the PCA-based feature extraction method outperforms the original method even when the training set is contaminated by scene details, and the proposed RSM can further improve it.

4. CONCLUSION

In the previous work [14], a feature extraction algorithm based on PCA denoising was proposed to extract a feature set with much lower dimensionality from the original noise residual. However, the performance of this algorithm degrades when scene details are contained in the training set, as the learned eigenvectors are affected by the scene details. As a result, the leading eigenvectors of the learned feature extractor is more likely to represent the scene details rather than the real SPN signal. Moreover, since scene details may differ for different training samples, it is hard to locate these corrupted eigenvectors in the entire feature space. To address these problems in this paper, an ensemble solution based on RSM and MV has been presented to randomly select subspaces from the PCA feature space to suppress the effect of scene details. The experimental results suggest that the proposed method has the capability to suppress the interference of scene details and achieves a superior ROC curve performance than both the original SPN extraction method and the PCA-based feature extraction method.

5. REFERENCES

[1] J. Lukas, J. Fridrich, and M. Goljan, "Digital camera identification from sensor pattern noise," *IEEE Trans. Inf. Forensics Security*, vol. 1, no. 2, pp. 205–214, 2006.

[2] K. Dabov, A. Foi, V. Katkovnik, and K. Egiazarian, "Image denoising by sparse 3d transform-domain collaborative filtering," *IEEE Trans. Image Process.*, vol. 16, no. 8, pp. 2080–2095, 2007.

[3] M. Chen, J. Fridrich, M. Goljan, and J. Lukas, "Determining image origin and integrity using sensor noise," *IEEE Trans. Inf. Forensics Security*, vol. 3, no. 1, pp. 74–90, 2008.

[4] C.-T. Li, "Source camera identification using enhanced sensor pattern noise," *IEEE Trans. Inf. Forensics Security*, vol. 5, no. 2, pp. 280–287, 2010.

[5] C.-T. Li and R. Satta, "Empirical investigation into the correlation between vignetting effect and the quality of sensor pattern noise," *IET Computer Vision*, vol. 6, no. 6, pp. 560–566, 2012.

[6] C.-T. Li and Y. Li, "Color-decoupled photo response non-uniformity for digital image forensics," *IEEE Trans. Circuits Syst. Video Technol.*, vol. 22, no. 2, pp. 260–271, 2012.

[7] X. Kang, J. Chen, K. Lin, and A. Peng, "A context-adaptive spn predictor for trustworthy source camera identification," *EURASIP Journal Image and Video Processing*, vol. 2014, no. 1, pp. 1–11, 2014.

[8] R. Li, C.-T. Li, and Y. Guan, "A reference estimator based on composite sensor pattern noise for source device identification," in *Proc. SPIE, Electronic Imaging, Media Watermarking, Security, and Forensics 2014*, San Francisco, CA, USA, Feb. 2-6, 2014, vol. 9028.

[9] M. Goljan, "Digital camera identification from images - estimating false acceptance probability," in *Proc. Int. Workshop Digital-forensics and Watermarking*, pp. 454–468. 2009.

[10] X. Kang, Y. Li, Z. Qu, and J. Huang, "Enhancing source camera identification performance with a camera reference phase sensor pattern noise," *IEEE Trans. Inf. Forensics Security*, vol. 7, no. 2, pp. 393–402, 2012.

[11] M. Goljan, J. Fridrich, and T. Filler, "Managing a large database of camera fingerprints," in *Proc. SPIE, Electronic Imaging, Media Forensics and Security XII*, San Jose, CA, USA, Jan. 17C21, 2010, vol. 7541, pp. 08 01–12.

[12] Y. Hu, C.-T. Li, and Z. Lai, "Fast source camera identification using matching signs between query and reference fingerprints," *Multimedia Tools and Applications*, pp. 1–24, 2014.

[13] S. Bayram, H. Sencar, and N. Memon, "Efficient sensor fingerprint matching through fingerprint binarization," *IEEE Trans. Inf. Forensics Security*, vol. 7, no. 4, pp. 1404–1413, 2012.

[14] R. Li, C.-T. Li, and Y. Guan, "A compact representation of sensor fingerprint for camera identification and fingerprint matching," in *Proc. IEEE Int. Conf. Acoustics, Speech, and Signal Processing*, Brisbane, Australia, Apr. 19-24, 2015, pp. 1777–1781.

[15] D. Zhang, R. Lukac, X. Wu, and D. Zhang, "PCA-based spatially adaptive denoising of CFA images for single-sensor digital cameras," *IEEE Trans. Image Process.*, vol. 18, no. 4, pp. 797–812, 2009.

[16] Y. Guan, C.-T. Li, and F. Roli, "On reducing the effect of covariate factors in gait recognition: A classifier ensemble method," *IEEE Trans. Pattern Anal. Mach. Intell.*, vol. 37, no. 7, pp. 1521–1528, July 2015.

[17] T. Gloe and R. Böhme, "The dresden image database for benchmarking digital image forensics," *Journal Digital Forensic Practice*, vol. 3, no. 2-4, pp. 150–159, 2010.